PHYSICAL REVIEW D **94,** 095017 (2016)

Natural supersymmetry from extra dimensions

A. Delgado,[1] M. Garcia-Pepin,[2] G. Nardini,[3] M. Quiros[2,4]

[1]*Department of Physics, University of Notre Dame, Notre Dame, Indiana 46556, USA*
[2]*Institut de Física d'Altes Energies (IFAE), The Barcelona Institute of Science and Technology (BIST), Campus UAB, 08193 Bellaterra (Barcelona), Spain*
[3]*Albert Einstein Center (AEC), Institute for Theoretical Physics (ITP), University of Bern, Sidlerstrasse 5, CH-3012 Bern, Switzerland*
[4]*Institució Catalana de Recerca i Estudis Avançats (ICREA), Campus UAB, 08193 Bellaterra (Barcelona), Spain*

(Received 29 August 2016; published 16 November 2016)

We show that natural supersymmetry can be embedded in a five-dimensional theory with supersymmetry breaking *à la* Scherk-Schwarz (SS). There is no "gluino-sucks" problem for stops localized in the four-dimensional brane and gluinos propagating in the full five-dimensional bulk, and sub-TeV stops are easily accommodated. The μ/B_μ problem is absent as well; the SS breaking generates a Higgsino Dirac mass, and no bilinear Higgs mass parameter in the superpotential is required. Moreover, for nonmaximal SS twists leading to $\tan\beta \simeq 1$, the Higgs spectrum is naturally split, in agreement with LHC data. The 125 GeV Higgs mass and radiative electroweak symmetry breaking can be accommodated by minimally extending the Higgs sector with $Y = 0$ $SU(2)_L$ triplets.

DOI: 10.1103/PhysRevD.94.095017

I. INTRODUCTION

In the past decades the hierarchy problem of the Standard Model (SM) has guided most of the particle physics community in the search for a UV completion able to describe nature up to the Planck (or Grand Unified Theory) cutoff scale. In this task, supersymmetry and compositeness have been, and still are, the most promising lighthouses to follow. Their most appealing feature is that their Higgs sectors are insensitive to the Planck mass cutoff, and are only sensitive to the scale of new physics which should, therefore, be close to the electroweak scale in order to avoid an (unnatural) *little* hierarchy problem. Despite this expectation, there is no sign of new physics in the LHC data. The situation is thus threatening: if the tendency in the data does not change, we might lose our trust in the naturalness criterion (and the subsequent loss of confidence on any deduction based on dimensional arguments), which would make our future way up to the Planck scale very hard. In order to avoid this threat, it is crucial to understand whether, and in case why, naturalness is hiding in the present LHC data.

In supersymmetry, several experimental observations seem to invoke a tuning in the electroweak sector. Indeed, if one does not rely on the low-energy corners of the parameter space still compatible with the experimental searches, a large gap between the soft-supersymmetry breaking and electroweak scales is required [1,2]. The tension between data and naturalness is, however, reduced and may be avoided, if there is a symmetry imposing some cancellations at both tree level and (at least) one loop.

The naturalness problem is manifest in the minimal supersymmetric extension of the SM (MSSM). In the MSSM the squared-mass term of the lighter CP-even (and SM-like) eigenstate h has the magnitude of the lighter eigenvalue in the matrix

$$\mathcal{M}^2_{H_1,H_2} = \begin{pmatrix} m_1^2 & m_3^2 \\ m_3^2 & m_2^2 \end{pmatrix}, \tag{1.1}$$

where $m_i^2 = (m_i^2)^0 + \Delta m_i^2$ contains radiative corrections Δm_i^2 to the desired order. The lightest eigenvalue of $\mathcal{M}^2_{H_1,H_2}$ thus needs to be $\mathcal{O}(m_Z^2)$ and negative to have agreement with the experimentally observed electroweak symmetry breaking (EWSB) pattern. The other Higgses, instead, with a squared mass of the order of the larger eigenvalue of $\mathcal{M}^2_{H_1,H_2}$, have to be hierarchically larger to avoid any tension with the extra-Higgs searches [3,4]. Two parameter regions seem promising for fulfilling these features:

(i) The so-called focus point solution [5–9], based on the fact that, for $m_1^2 \gg m_3^2$, or equivalently $\tan\beta \gg 1$, $\mathcal{M}^2_{H_1,H_2}$ is essentially diagonal. In this case no tree-level tuning is required if $m_2^2 \sim \mathcal{O}(-m_Z^2)$.

(ii) The parameter region $m_1^2 \simeq m_2^2 \simeq m_3^2 \gg \mathcal{O}(m_Z^2)$ (equivalent to $\tan\beta \simeq 1$) which, if justified by a symmetry, naturally leads to a vanishing eigenvalue in $\mathcal{M}^2_{H_1,H_2}$.

However, several issues jeopardize the naturalness of these two options. In particular, the supersymmetric parameter μ[1] cannot be below the electroweak

[1]This parameter provides a supersymmetric contribution to the tree-level Higgs masses $(m_{1,2}^2)^0 = m_{H_{1,2}}^2 + \mu^2$.

scale because of the lightest chargino mass bound, $m_{\tilde{\chi}^\pm} \gtrsim 105$ GeV [10]. Moreover, even if μ is above this bound, it can be in tension with the general electroweakino searches, depending on the gaugino mass spectrum [11,12]. Finally if all these constraints are circumvented, still, explaining theoretically why the electroweak scale appears naturally in the superpotential is challenging.

The radiative corrections Δm_i^2 should also lift concerns. They should be small in order not to introduce a tuning at one loop. In this sense, the charged sleptons and bottom squarks that must be heavy to fulfill the flavor constraints [13] are innocuous when $\tan\beta$ is not huge. Stop contributions are instead dangerous. Thus, naturalness requires light stops, which are in agreement with top squark searches and 125 GeV Higgs mass constraints only in the presence of heavy gluinos and sizable stop mixing [14–16]. Unfortunately, the latter also generate large radiative corrections that need to be tuned, while the former tend to be inconsistent with light stops in top-down approaches. In fact, heavy gluinos pull the stop soft masses above the TeV scale along the running from the scale at which they are generated (if this scale is large enough) to the electroweak scale [17].

In view of the above issues, an appropriate strategy to resurrect naturalness in the present LHC data may consist in looking for UV embeddings where

(i) The tree-level Higgs mass is higher than in the ("vanilla") MSSM in such a way that rather light stops with negligible mixing are viable.
(ii) Gluinos are heavy, but the scale at which the soft stop masses are generated, and below which the renormalization-group (RG) evolution applies, is rather low (i.e. stop masses remain small while running down to the electroweak scale).
(iii) In the superpotential no mass term is required, so that the Dirac mass of the Higgsinos does *not* have a superpotential origin.

Remarkably, the five-dimensional (5D) $N = 1$ supersymmetry embeddings of Refs. [18,19] can fulfill these requirements [20,21]. When the fifth dimension is compactified on the circle orbifold $S_1/\mathbb{Z}_2$ of radius R, the $N = 1$ chiral superfields propagating in the bulk receive soft supersymmetry-breaking scalar masses and/or Dirac fermionic masses, depending on some global charge assignments technically called Scherk-Schwarz (SS) twists [22,23]. It is then possible to arrange the 5D Higgs sector in bulk chiral superfields in such a way that, below the compactification scale, the four-dimensional (4D) effective theory is equivalent to the MSSM with either $\tan\beta = 1$ [with $m_1^2 = m_2^2 = m_3^2 \sim \mathcal{O}(1/R^2)$ exact at tree level] for nonmaximal twists [19–21] or $\tan\beta = \infty$ for maximal twists [24,25]. Crucially, no contribution mimicking a superpotential squared mass μ^2 arises, although the Higgsinos do receive an $\mathcal{O}(1/R)$ Dirac mass, as required by condition (iii).[2]

This supersymmetry breaking mechanism, dubbed the SS mechanism [22], also works on vector superfields. It naturally leads to a spectrum where all gauge bosons are massless (prior to EWSB) and all gauginos have $\mathcal{O}(1/R)$ Majorana masses. On the other hand, at tree level, it does not induce any supersymmetry breaking for superfields localized at a brane of the orbifold. Therefore, by assuming a localized third generation of squarks, the stop soft squared masses are generated with a suppression of a one-loop factor.[3] Moreover, since the logarithmic ratio between the electroweak scale and the compactification scale (at which the SS mechanism induces supersymmetry breaking) is small, the stop masses are not drastically modified by their RG evolution and remain $\mathcal{O}(0.1/R)$, as required by condition (ii). Finally, also the requirement (i) can be fulfilled. In (maximally twisted) SS scenarios leading to $\tan\beta = \infty$, 5D nonminimal supersymmetric extensions with one singlet on the brane, or two pairs of vectorlike fermions on the brane, or an extra $U(1)'$ vector superfield in the bulk, boost the tree-level mass of the SM-like Higgs [24,25].[4]

The 5D SS scenarios then contain all the ingredients guaranteeing the SM-like Higgs squared-mass term to be $\mathcal{O}(m_Z^2)$, provided by gauge interactions without an unnatural tuning. The last obstacle is the sign of this term. In fact, in the above SS scenarios solving the issue (i), EWSB (namely with a negative sign in the Higgs squared mass term) can be achieved only by means of higher-dimensional operators whose magnitude and origin are hard to identify. It is then worth proving that there exist SS scenarios where these operators are not necessary for a successful EWSB, and where, at the same time, the requirements (i), (ii), and (iii) are fulfilled. We achieve this result by focusing on minimal extensions of the chiral superfield sector (for a study where the EWSB is obtained in nonminimal chiral extensions violating condition (iii); see Ref. [26]). We also restrict ourselves to the orbifold charge assignments corresponding to the $\tan\beta = 1$ case, for which the F terms contributions to the Higgs tree-level mass are enhanced.

Our proof of principle is developed in several steps. In Sec. II we review how to embed the MSSM in a 5D SS scenario and why the 125 GeV Higgs mass and the EWSB are problematic. Since the former problem should be

[2]Notice that also the chiral superfields associated with the first and second generations of squarks and sleptons will benefit from the same supersymmetry breaking if these superfields propagate in the bulk. There exist charge assignments for which their fermions are massless (prior to EWSB) but their superpartners are at the $\mathcal{O}(1/R)$ scale. This makes the SS mechanism naturally compatible with the flavor constraints [13].

[3]The stop mixing is also suppressed by a loop factor and is far away from the maximal mixing value as discussed in Sec. II.

[4]At a quantitative level, the singlet case might be problematic as its F-term contribution to the Higgs quartic coupling is suppressed at large $\tan\beta$.

trivially avoidable in a MSSM 5D scenario supplemented by a singlet, we consider in Sec. III the case where there is an extra singlet chiral superfield localized at the brane. As expected, the Higgs mass bound can be accommodated, but the radiative corrections to the SM-like squared-mass term are not sufficient to trigger the EWSB, analogously to the $\tan\beta = \infty$ case [24,25]. In addition, and surprisingly previously unnoticed, as the singlet is not protected by any symmetry of the theory, it develops a large tadpole (prior to the EWSB) inducing a $\mathcal{O}(1/R)$ vacuum expectation value (VEV) to the singlet. This jeopardizes the treatment of the Higgs Kaluza-Klein (KK) towers and the possibility of achieving Higgs-singlet mixings compatible with the LHC constraints [27]. This VEV could of course be suppressed by introducing a (huge) singlet mass term in the superpotential.[5] Since this possibility would violate the criterion (iii), and moving the singlet to the bulk should not circumvent the problem, in Sec. IV we pursue the analysis with the $Y = 0$ $SU(2)_L$-triplet extension of the MSSM, in which case the gauge symmetry itself forbids the large tadpole. This case, with the 5D $N = 1$ triplet superfield being in the bulk—triplet charginos would be too light if the superfield were localized on the brane—turns out to be the example of SS scenario that satisfies all the requests of our proof. Finally, in Sec. IV E we discuss some further phenomenological bounds and the need for localizing on the brane the third family of the leptonic superfield to overcome the dark matter bound, and in Sec. V we present our conclusions.

II. 5D MSSM

We embed the MSSM in a 5D space-time setup where the extra dimension is the orbifold $S^1/\mathbb{Z}_2$ with two 4D branes at the fixed points $y = 0$ and $y = \pi R$ (R is the radius of the circle S^1). The gauge and Higgs sectors, as well as the first and second generations of matter (and the right-handed stau[6]), propagate in the bulk while the rest of the third generation matter is localized at the $y = 0$ brane. The boundary conditions of the bulk fields are twisted by introducing SS parameters associated with the available global symmetries we are allowed to break. In this section we present a summary of the formalism and results in the MSSM (nonminimal extensions are considered in Secs. III and IV). The original calculations were performed mainly in Refs. [19–21] to which we will refer for more details. To simplify the notation, hereby, unless explicitly stated, we use units where $R \equiv 1$.

In 5D supersymmetry the Higgs doublets in the bulk belong to the $N = 2$ hypermultiplets $\mathbb{H}_a = (H_a, H_a^c, \Psi_a, F_a, F_a^c)$ (with $a = 1, 2$), where H_a and H_a^c are complex $SU(2)_L$ doublets with hypercharge $1/2$ and $\Psi_a = (\psi_a, \bar{\psi}_a^c)^T \equiv (\psi_{aL}, \psi_{aR})^T$ are $SU(2)_L$-doublet Dirac spinors with ψ_a ($\bar{\psi}_a$) and ψ_a^c ($\bar{\psi}_a^c$) being undotted (dotted) Weyl spinors. The two hypermultiplets $\mathbb{H}_a$ have the same quantum numbers and can then be arranged to form a doublet of a global symmetry, $SU(2)_H$, acting on the index a. The doublet of $N = 2$ hypermultiplets can also be split into $\mathbb{Z}_2$ even and odd $N = 1$ chiral multiplets according to the $\mathbb{Z}_2$ parity assignment

$$\mathbb{Z}_2 = \sigma_3|_{SU(2)_H} \otimes \gamma_5, \tag{2.1}$$

where σ_3 acts on the $SU(2)_H$ indices and γ_5 over Dirac indices. For $\mathbb{H}_1$ and $\mathbb{H}_2$, we take (H_2, ψ_{2L}, F_2) and (H_1, ψ_{1R}, F_1) to be even and $(H_2^c, \psi_{2R}, F_2^c)$ and $(H_1^c, \psi_{1L}, F_1^c)$ to be odd.

The gauge sector in the bulk is instead described by $N = 2$ vector supermultiplets. For a $SU(N)$ gauge group each of the supermultiplets is given by $\mathbb{V} = (V_M, \lambda_L^i, \Upsilon)$, which contains the vector bosons V_M (with $M = 1, \ldots, 5$), the real scalar Υ, and the two bispinors λ_L^i (with $i = 1, 2$). All these fields are in the adjoint representation of $SU(N)$. As customary we assume V_μ and λ_L^1 (V_5,Υ, and λ_L^2) to be even (odd) with respect to the $\mathbb{Z}_2$ symmetry.

The SS twists (q_R, q_H) associated with the global symmetries $SU(2)_R \times SU(2)_H$ impose the relation

$$\begin{bmatrix} H_1(x,y) & H_1^c(x,y) \\ H_2^c(x,y) & H_2(x,y) \end{bmatrix} = e^{iq_H\sigma_{2y}} \sum_{n=0}^{\infty} \sqrt{\frac{2}{\pi}} \begin{bmatrix} \cos nyH_1^{(n)}(x) & \sin nyH_1^{c(n)}(x) \\ \sin nyH_2^{c(n)}(x) & \cos nyH_2^{(n)}(x) \end{bmatrix} e^{-iq_R\sigma_{2y}}, \tag{2.2}$$

where $H_{1,2}^{(n)}(x)$ (with $n \geq 0$) and $H_{1,2}^{c(n)}(x)$ (with $n \geq 1$) are the KK modes of the corresponding doublets (their x dependence is omitted hereafter) and have mass dimension equal to one. The $\sqrt{2/\pi}$ factor comes from the normalization of the nonzero modes in the interval $[0, \pi]$. The zero modes $H_a^{(0)}$ are then *not* canonically normalized as they are missing a prefactor $1/\sqrt{2}$. The mass doublet eigenstates $h^{(n)}$ and $H^{(n)}$, with masses $q_R - q_H + n$ and $q_R + q_H + n$, respectively (with n from $-\infty$ to $+\infty$), are computed in Ref. [19]. They are given by

$$\begin{aligned} H_1^{(n)} &= (h^{(n)} + h^{(-n)} + H^{(n)} + H^{(-n)})/2, \\ H_2^{(n)} &= (h^{(n)} + h^{(-n)} - H^{(n)} - H^{(-n)})/2, \\ H_1^{c(n)} &= (h^{(-n)} - h^{(n)} + H^{(-n)} - H^{(n)})/2, \\ H_2^{c(n)} &= (h^{(n)} - h^{(-n)} + H^{(-n)} - H^{(n)})/2, \end{aligned} \tag{2.3}$$

for $n \geq 1$, and by

[5]This term was considered in e.g. Ref. [26] to suppress the effect of the tadpole estimated to be of the order of the electroweak scale.

[6]We are considering $\tilde{\tau}_R$ propagating in the bulk in order to avoid bounds on heavy stable charged particles [28].

$$H_1^{(0)} = (h^{(0)} + H^{(0)})/2,$$
$$H_2^{(0)} = (h^{(0)} - H^{(0)})/2, \quad (2.4)$$

for $n = 0$. Notice that although $H_a^{(0)}$ are noncanonically normalized, the zero modes $h^{(0)}$ and $H^{(0)}$ are canonically normalized, which has enforced the introduction of an extra factor of $1/\sqrt{2}$ in Eq. (2.4). In this way, even though the zero modes are differently normalized than the nonzero ones, it is straightforward to reconstruct full KK towers (with n from $-\infty$ to $+\infty$) of fields when coupled to the brane. As for the Higgsino components in $\mathbb{H}_a$, the mass eigenstates are (for $n > 0$)

$$\tilde{H}^{(-n)} = \frac{1}{\sqrt{2}}(\psi_2^{(n)} - \gamma_5\psi_1^{(n)}), \qquad \text{with mass}(q_H - n),$$
$$\tilde{H}^{(+n)} = \frac{1}{\sqrt{2}}(\gamma_5\psi_2^{(n)} + \psi_1^{(n)}), \qquad \text{with mass}(q_H + n),$$
$$\tilde{H}^{(0)} = (\psi_{2L}^{(0)}, \psi_{1R}^{(0)})^T, \qquad \text{with mass}(q_H). \quad (2.5)$$

The $SU(2)_R$ twist also acts on all bulk gauginos, which are embedded in $\mathbb{V}_j$. The KK tower of these fields have Majorana masses $n + q_R$. Moreover, any field in the bulk coupled to these charginos is sensitive to the twist q_R. All bulk matter fields have, in fact, a KK tower with tree-level masses $n + q_R$ for scalars and n for fermions. Bulk fields that are $SU(2)_R$ singlets (e.g. the gauge vector bosons and scalars of $\mathbb{V}_j$), or fields in the brane, are instead insensitive to q_R and their spectrum is not affected by the SS mechanism.[7]

The scenario with charges $q_R = q_H \equiv \omega$ is particularly interesting. The doublet $h^{(0)}$ is massless while the doublet $H^{(0)}$ has mass 2ω. The corresponding KK modes, $h^{(n)}$ and $H^{(n)}$, have masses n and $2\omega + n$, respectively. Higgsinos and charginos have masses $\omega + n$. The first and second generation sfermions and right-handed staus, which we assume in the bulk, also have mass eigenstates $\omega + n$, while their supersymmetric partners have masses n. In the rest of the paper we focus on this scenario and some minimal extensions of it.

The main features of this scenario are the following:

(i) The Higgsino zero mode has a Dirac mass equal to ω/R, by which there is no need to introduce a superpotential μ-like term as in the MSSM. *The μ-problem is thus naturally solved by this formalism.*

(ii) At tree level the theory predicts a 4D massless Higgs doublet with a flat potential [19]. The rest of the Higgs sector is heavy. In the MSSM language this amounts to equations of electroweak minimum with $\tan\beta = 1$ and invariant under the global scale change $\omega/R \to \lambda\omega/R$. Such an invariance reminds some of the properties of the focus point solution [5–8].

(iii) States localized in the brane, i.e. third generation of squarks and third generation of slepton doublet, are naturally light as their tree-level masses are vanishing. Their one-loop radiative masses from KK modes are finite [21] and can be interpreted as finite threshold effects after integrating out the heavy modes. Moreover, left-handed and right-handed squarks do not mix much as their mixings are generated only at one loop as well. The values of the stop mixing A_t and the one-loop masses of the fields localized in the brane are displayed in Fig. 1 (their explicit expressions are given in Ref. [21]).

(iv) The lightest ($n = 0$) modes of the fields in the bulk have tree-level masses that are zero, ω/R, $2\omega/R$, or $1/R$. Those with vanishing masses correspond to SM-like fields. The new-physics spectrum thus exhibits very compressed sectors, with a large gap between new-physics bulk and brane states. In this way the first and second generation sfermions, and the right-handed staus as well, are naturally much heavier than the stops, sbottoms, and left-handed staus and tau sneutrinos, in agreement with flavor constraints. The explicit values of the lightest new-physics modes are presented in Fig. 2.

(v) The EWSB has to proceed by radiative corrections as discussed here below.

The minimal picture suffers then from two drawbacks:

(i) **EWSB**: In this theory the radiative corrections to the mass terms are known [19–21]. They are finite and can be considered as threshold effects at the compactification scale $\mathcal{O}(1/R)$ at which all heavy bulk fields are integrated out. In particular, at one loop, there are gauge corrections to the squared mass of the SM Higgs (m^2) and the brane fields $\tilde{Q}_{3L}, \tilde{U}_{3R}, \tilde{D}_{3R}, \tilde{E}_{3R}$ ($m_Q^2, m_U^2, m_D^2, m_E^2$), which are positive, thus preventing EWSB. As stops are localized, and massless at tree level, they do not produce any *one-loop* correction to the Higgs mass proportional to h_t^2 which could trigger EWSB as in the 4D MSSM. Of course, when they are integrated out, they generate a (logarithmic) radiative correction depending on their own (one-loop) masses: a two-loop effect. In the $\overline{\text{MS}}$ scheme this correction is given by [9]

$$\Delta m^2 = \frac{6h_t^2}{32\pi^2}[G(m_Q^2) + G(m_U^2)] + 6h_t^2A_t^2\frac{G(m_Q^2) - G(m_U^2)}{m_Q^2 - m_U^2},$$
$$G(x) \equiv x^2\left(\log\frac{x^2}{\mathcal{Q}^2} - 1\right). \quad (2.6)$$

To leading order in α_3 it turns out that $m_Q(\omega) = m_U(\omega)$, and Eq. (2.6) becomes

[7]For our twist assignments, each bosonic component $V_\mu^j, V_5^j, \Upsilon^j$ of $\mathbb{V}^j$ exhibits a KK spectrum with masses n, and both V_5 and Υ have vanishing zero modes.

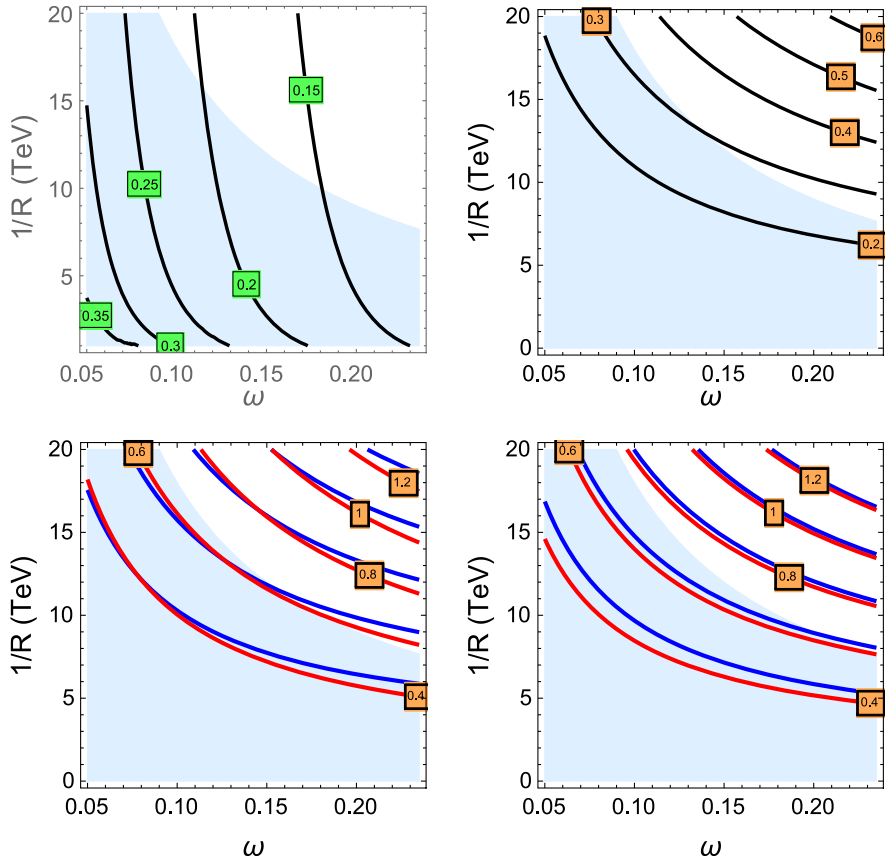

FIG. 1. Contour plots of the most relevant loop-induced parameters. In light blue the region with gluino mass $m_{\tilde{g}} < 1.8$ TeV, in tension with LHC bounds (see Sec. IV E). Mass labels are in TeV units. Upper left panel: Stop trilinear parameter normalized as $X_t = A_t/m_Q$. Upper right panel: Masses of the scalar left-handed tau $\tilde{\tau}_L$ and the scalar left-handed tau neutrino $\tilde{\nu}_\tau$. Lower left panel: Masses of the lightest states of the stop $\tilde{t}_1$ and sbottom $\tilde{b}_1$ (red and blue lines, respectively). Lower right panel: Masses of the heaviest states of the stop $\tilde{t}_2$ and sbottom $\tilde{b}_2$ (red and blue lines, respectively).

$$\Delta m^2 = -\frac{3h_t^2}{8\pi^2} m_Q^2(\omega)\left(\log\frac{\mathcal{Q}^2}{m_Q^2} + 1\right). \qquad (2.7)$$

In Eq. (2.7) we can set the renormalization scale $\mathcal{Q}$ at the scale where the boundary conditions are imposed, i.e. where the theory becomes 4D. In Ref. [19] it was taken as $\mathcal{Q} \simeq \omega/R$, whereas in Ref. [24] it was fixed as $\mathcal{Q} \simeq 1/(\pi R)$. In both cases the two-loop correction coming from m_Q^2, m_U^2, and A_t^2, which are generated only at one loop, are too

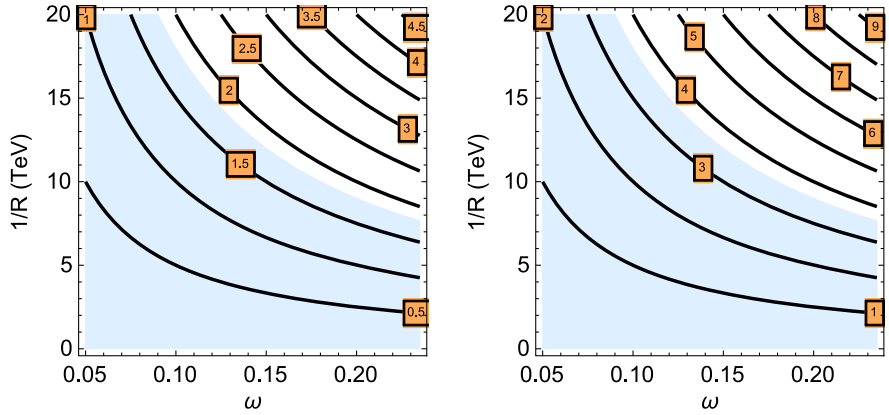

FIG. 2. Contour plots of the tree-level masses of the bulk fields sensitive to the SS mechanism. Labels are in TeV units. Left panel: First and second generation sfermions, right-handed stau, gauginos, and Higgsinos. Right panel: Charged and neutral heavy doublet Higgses. Blue areas are as in Fig. 1.

small to drive $m^2 < 0$. On the other hand, the choice of $\mathcal{Q}$ in Eq. (2.7) only concerns the scale dependence in the three-loop contribution.[8] Since we are not calculating all consistent two-loop effects (e.g. we integrate out the heavy KK modes only at one loop), our EWSB analysis should not rely on just the few two-loop pieces that are known, and which do not change either qualitatively or quantitatively the EWSB picture, as we have checked. Thus, to be consistent, we consider the EWSB at one loop, and hereafter we will then ignore all two-loop EWSB contributions as the one in Eq. (2.7).

(ii) **Higgs mass**: As both stop soft masses and trilinear stop mixing parameter are one-loop suppressed, their radiative correction to the Higgs quartic coupling is too small to reproduce the experimental value $m_h \simeq 125$ GeV. This problem was already recognized in the early papers [19–21] and has been more recently revamped [24,25].

In Ref. [24] problem (i) was solved by the introduction of higher dimensional operators, while problem (ii) was milder; as for the maximal SS breaking case $\omega = 1/2$ the equations of motion lead to $\tan\beta = \infty$, and are solved by introducing an extra $U(1)$ factor. In Ref. [26] both problems were addressed by adding a singlet plus a folded sector (i.e. a copy of the matter superfields) at the expense of bilinear mass term parameters in the superpotential. In the present paper we will see that an extended Higgs sector can solve both problems without violating the requirements (i), (ii), and (iii) of Sec. I. As an extra singlet is appropriate to add tree-level corrections (an F-term contribution) to the Higgs mass in the case of $\tan\beta = 1$, we will first start considering the case of a localized singlet.

III. 5D MSSM PLUS A SINGLET

Our setup in this section will be identical to that of Sec. II but with the addition of a singlet. For simplicity we will first consider the case of a singlet field S localized on the $y = 0$ brane.

A. Embedding and 4D Lagrangian

A singlet localized on the $y = 0$ brane admits a superpotential interaction with the (bulk) Higgs multiplets that can be derived from the brane superpotential

$$W = \hat{\lambda}\mathcal{H}_1 \cdot \mathcal{H}_2 S\delta(y), \tag{3.1}$$

where $\hat{\lambda}$ is a 5D Yukawa coupling with mass dimension equal to -1. Specifically, only the even Higgs components couple to the fields on the $y = 0$ brane, so that the corresponding $N = 1$ superfields $\mathcal{H}_1$ and $\mathcal{H}_2$ are given by [29]

$$\begin{aligned}\mathcal{H}_2 &= (H_2, \psi_{2L}, F_2 - \partial_5 H_2^c),\\ \mathcal{H}_1 &= (\tilde{H}_1, \tilde{\psi}_{1R}, \tilde{F}_1 - \partial_5 \tilde{H}_1^c),\end{aligned} \tag{3.2}$$

where, for a doublet A with hypercharge $1/2$, $\tilde{A} = -i\sigma_2 A^\star$ stands for a doublet with hypercharge $-1/2$. In particular, the fermionic components of $\mathcal{H}_{1,2}$ interact with the singlet as a Dirac fermion Ψ defined as [cf. Eq. (2.5)]

$$\begin{aligned}\Psi &= \sum_{n=0}^{\infty}\psi^{(n)} \equiv \sum_{n=0}^{\infty}\begin{pmatrix}\psi_{2L}^{(n)}\\ \psi_{1R}^{(n)}\end{pmatrix}\\ &= \tilde{H}^{(0)} + \frac{1}{\sqrt{2}}\sum_{n=1}^{\infty}(\tilde{H}^{(n)} + \tilde{H}^{(-n)}) \equiv \frac{1}{\sqrt{2}}\tilde{H}.\end{aligned} \tag{3.3}$$

In fact, from Eqs. (3.1) and (3.2) one can determine the 4D Lagrangian. After integrating out the auxiliary fields, its bosonic part reads

$$\begin{aligned}\mathcal{L}_4 = &-\hat{\lambda}S\{\partial_5 H_1^{c\dagger}(0)H_2(0) + H_1^\dagger(0)\partial_5 H_2^c(0) + \text{H.c.}\}\\ &- \hat{\lambda}^2\{|H_1(0)^\dagger H_2(0)|^2 + |S|^2(|H_1(0)|^2\\ &+ |H_2(0)|^2)\pi\delta(0)\},\end{aligned} \tag{3.4}$$

with

$$\delta(0) \equiv \frac{1}{\pi}\sum_{n=-\infty}^{\infty} 1. \tag{3.5}$$

Moreover, using the notation

$$h = \sum_{n=-\infty}^{\infty} h^{(n)}, \qquad \hat{h} = \sum_{n=-\infty}^{\infty}(q_R - q_H + n)h^{(n)}, \tag{3.6}$$

$$H = \sum_{n=-\infty}^{\infty} H^{(n)}, \quad \hat{H} = \sum_{n=-\infty}^{\infty}(q_R + q_H + n)H^{(n)}, \tag{3.7}$$

then

$$\begin{aligned}\partial_5 H_1^c(0) &= \frac{-1}{\sqrt{2\pi}}(\hat{h} + \hat{H}), \qquad H_1(0) = \frac{1}{\sqrt{2\pi}}(h + H),\\ \partial_5 H_2^c(0) &= \frac{1}{\sqrt{2\pi}}(\hat{h} - \hat{H}), \qquad H_2(0) = \frac{1}{\sqrt{2\pi}}(h - H),\end{aligned} \tag{3.8}$$

and Eq. (3.4) reads

[8]Note that the EWSB could be determined by means of the RG-improved effective potential. In that case the resulting EWSB condition is independent of $\mathcal{Q}$ at a given perturbative order [9]. The choice of $\mathcal{Q}$ is then only aimed to minimize the corrections coming at the next perturbative order.

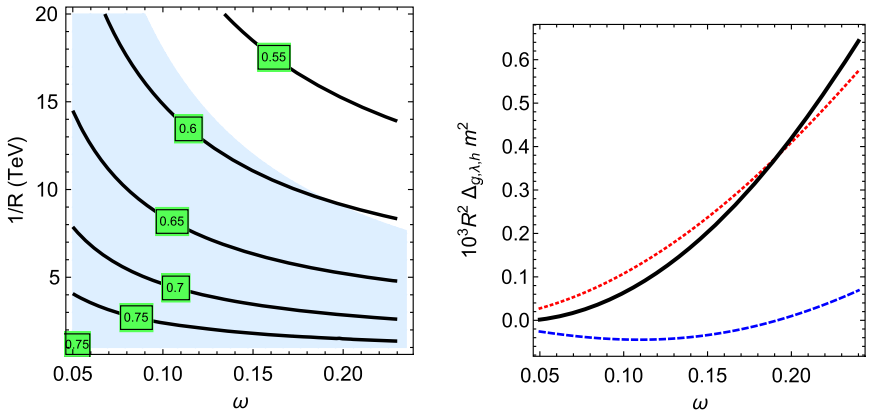

FIG. 3. Left panel: Contour plot of values of λ leading to the experimental value $m_h = 125$ GeV if the observed EWSB is achieved. Blue area is as in Fig. 1. Right panel: Plot of $10^3R^2\Delta_g m^2$ (red dotted line), $10^3R^2\Delta_\lambda m^2$ (blue dashed line), and its sum $10^3R^2\Delta_h m^2$ (black solid line), for $1/R = 2$ TeV and λ fixed from the plot on the left panel, as a function of ω.

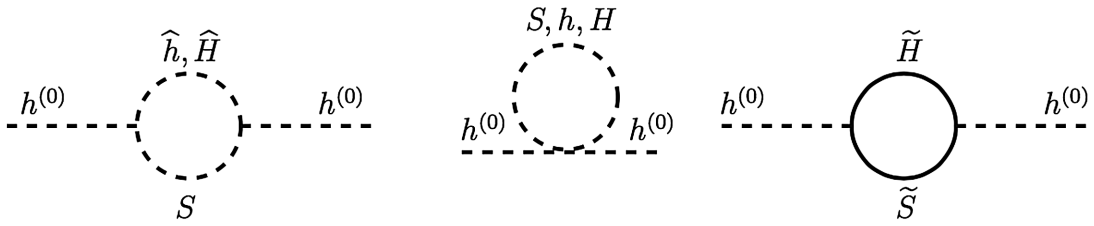

FIG. 4. Diagrams contributing to the correction $\Delta_\lambda m^2$ to the squared-mass term of $h^{(0)}$.

$$\mathcal{L}_4 = -\frac{\lambda}{2}\{S(h^\dagger + H^\dagger)(\hat{h} - \hat{H}) - S^\dagger(h^\dagger - H^\dagger)(\hat{h} + \hat{H}) + \text{H.c.}\} - \lambda^2\left\{\frac{1}{4}||h|^2 - |H|^2 - h^\dagger H + H^\dagger h|^2 + |S|^2(|h|^2 + |H|^2)\pi\delta(0)\right\}, \tag{3.9}$$

where $\lambda \equiv \hat{\lambda}/\pi$ is the (dimensionless) 4D Yukawa coupling.

B. Quartic and quadratic terms of the lightest Higgs

As we can see from Eq. (3.9), the coupling λ is the tree-level source of the $h^{(0)}$ quartic coupling. The $h^{(0)}$ potential is then given by

$$V_{\text{SM}} = (m^2 + \Delta_h m^2)|h^{(0)}|^2 + \left(\frac{\lambda^2}{4} + \Delta\lambda\right)|h^{(0)}|^4 + \ldots, \tag{3.10}$$

where m^2 is the tree-level Higgs squared mass term while $\Delta_h m^2$ and $\Delta\lambda$ are the radiative contributions to the Higgs mass and quartic coupling, respectively.

We determine the total $h^{(0)}$ quartic coupling at leading order in λ and h_t. Since the λ dependence already appears at tree level, $\Delta\lambda$ is the usual MSSM radiative correction [30]

$$\Delta\lambda = \frac{3m_t^4}{8\pi^2 v^4}\left[\log\frac{m_{\tilde{t}}^2}{m_t^2} + \frac{A_t^2}{m_{\tilde{t}}^2}\left(1 - \frac{A_t^2}{12m_{\tilde{t}}^2}\right)\right], \tag{3.11}$$

in which $v = 174$ GeV (i.e. where the observed EWSB is assumed). Notice that as both $m_{\tilde{t}}^2 \simeq m_U^2 \simeq m_Q^2$ and A_t are generated at one loop by exchange of KK modes (see e.g. Ref. [19]), $\Delta\lambda$ is a two-loop effect. Moreover, if we assume $m^2 + \Delta_h m^2 \simeq -(88\text{ GeV})^2$, in agreement with the EWSB observations, Eqs. (3.10) and (3.11) can be used to translate the constraint on the $h^{(0)}$ scalar mass, m_h, into λ. This is quantified in Fig. 3 (left panel) where the explicit values of λ providing $m_h = 125$ GeV are displayed as a function of $1/R$ and ω, with the correction $\Delta\lambda$ being included.

On the other hand, it is not obvious that the EWSB condition $m^2 + \Delta_h m^2 \simeq -(88\text{ GeV})^2$ can be fulfilled. As discussed in Sec. II, m^2 is vanishing. The EWSB then relies only on the loop-induced quantity $\Delta_h m^2$. This can be split as $\Delta_h m^2 = \Delta_g m^2 + \Delta_\lambda m^2$, where $\Delta_g m^2$ and $\Delta_\lambda m^2$ are the contributions depending, respectively, on the $SU(2)_L$ gauge coupling g and on the superpotential parameter λ.[9] The quantity $\Delta_g m^2$ amounts to [19]

$$\Delta_g m^2 = \frac{g^2}{64\pi^4}[9\Omega(0) + 3\Omega(2\omega) - 12\Omega(\omega)] \tag{3.12}$$

[9]For simplicity we are neglecting here the subleading contribution corresponding to the $U(1)_Y$ gauge interactions.

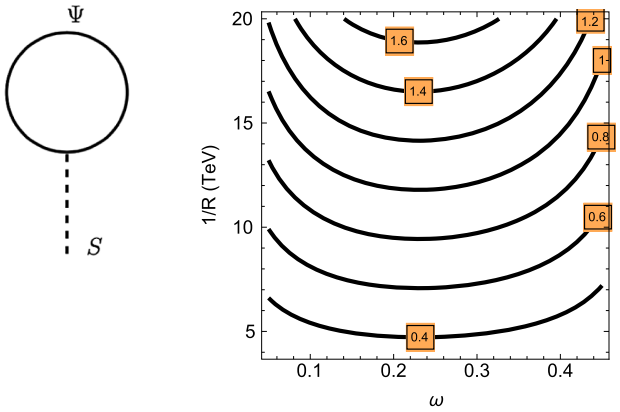

FIG. 5. Left panel: Diagrams contributing to the tadpole of S. Right panel: Contour plot of the triplet trilinear parameter $\xi^{1/3}(\omega, 1/R)$ with λ adjusted to reproduce the observed Higgs mass. Labels are in TeV units.

with

$$\Omega(\omega) = \frac{1}{2}[Li_3(e^{2i\pi\omega}) + Li_3(e^{-2i\pi\omega})](1/R)^2. \quad (3.13)$$

The contribution $\Delta_\lambda m^2$ is generated by the diagrams in Fig. 4 and turns out to be

$$\Delta_\lambda m^2(\omega) = \frac{\lambda^2}{32\pi^4}[\Omega(0) + \Omega(2\omega) - 2\Omega(\omega)]. \quad (3.14)$$

Plots of $\Delta_g m^2$, $\Delta_\lambda m^2$, and $\Delta_h m^2$ as a function of ω are shown in the right panel of Fig. 3. In the plots the value of λ is adjusted to reproduce the Higgs mass constraint (cf. left panel of Fig. 3) assuming that EWSB occurs. A representative value of R is assumed, namely $1/R = 2$ TeV. For this illustrative case it results that $\Delta_\lambda m^2$, although negative for $0 \lesssim \omega \lesssim 0.2$, is insufficient to overcome the positive contribution $\Delta_g m^2$ and drive $\Delta_h m^2$ to negative values. We check that this negative result is generic.

We conclude that in the 5D MSSM plus a localized singlet, the extra field content helps in reproducing the experimental value of the Higgs mass but does not seem to improve the scenario from the EWSB problem. A possible solution is to introduce higher-dimensional operators as in Ref. [24]. However, a subtlety in the analysis might be exploited to circumvent the problem: if there is sizable mixing between the singlet and Higgs scalars, $\Delta_h m^2$ is not the unique quantity playing a role in the EWSB. We sketch the features of this possibility in the following section.

C. Tadpole and VEV of the singlet

The interaction between the singlet and the fermions of $\mathcal{H}_{1,2}$ allows the Feynman diagram of Fig. 5 (left panel) to generate the linear term in the Lagrangian proportional to S, as it is not protected by any symmetry of the theory. Then there exists a tadpole term in the localized Lagrangian as

$$\mathcal{L}_4 = -\xi(\omega, 1/R)(S + S^\dagger) + \cdots. \quad (3.15)$$

The coefficient of this interaction is expected to be sizable.[10] Indeed, the sum of the contributions of each KK mode $\psi^{(n)}$ yields

$$\xi(\omega, 1/R) = \frac{3i}{32\pi^5}[Li_4(e^{-2i\pi\omega}) - Li_4(e^{2i\pi\omega})](1/R)^3, \quad (3.16)$$

and its numerical value can be deduced from the right panel of Fig. 5. The size $\mathcal{O}(0.1/R)$ is then expected to be the natural scale of the dimensionful parameters involved in the singlet potential, so that the VEV that is eventually acquired by the singlet should be parametrically $\mathcal{O}(1\text{ TeV})$ for $1/R \sim 10$ TeV. The fields $h^{(0)}$ and S can thus have a non-negligible mixing. In principle the mixing could help the implementation of the EWSB at the expense of some tension with the Higgs signal strengths measured at the LHC [27].[11] Determining whether these possibilities are not ruled out by the present LHC data would need a dedicated analysis that goes beyond the scope of the present paper, and in any case we do not expect the surviving parameter region to be really promising concerning naturalness. On the other hand, the situation would not radically change by considering singlets in the bulk, as bulk singlets still acquire a large VEV. We thus focus the rest of our analysis on the 5D MSSM extended by hyperchargeless $SU(2)_L$ triplets for which tadpoles prior to the EWSB are forbidden by the gauge symmetry.

IV. 5D MSSM PLUS BULK TRIPLETS

We consider the scenario where the Higgs sector is extended by hyperchargeless $SU(2)_L$ triplets. In the context of 4D supersymmetry the model is somewhat well known (see e.g. Refs. [31–38]), but its implementation in a 5D framework has not been attempted yet. In this section we implement it in a SS scenario. As we refrain from introducing any dimensionful parameter in the 4D superpotential, we do not consider the option of triplets localized on the brane (in which case the fermionic triplet components would be too light to overcome the chargino mass bound $m_{\tilde{\chi}^\pm} \gtrsim 104$ GeV [10]). We thus consider the 5D MSSM extensions with triplets propagating in the bulk.

[10]This contribution has not been noticed in the previous literature. The recent proposals [25,26] might be affected by this tadpole term.

[11]Although $h^{(0)}$ and S have positive (one-loop) squared-mass terms, there may be a linear combination developing a negative quadratic term thanks to the mixing.

A. Embedding and 4D Lagrangian

Similar to the case of bulk doublets (see Sec. II), the bulk triplets can be arranged in $Y=0$ $SU(2)_L$-triplet hypermultiplets $\mathbb{T}_b=(\Sigma_b,\Sigma_b^c,\Psi_{\Sigma_b},F_{\Sigma_b},F_{\Sigma_b})$ with $b=1,\ 2$, which transform as a doublet under the global bulk group $SU(2)_\Sigma$ acting on the index b. The fermionic component $\Psi_{\Sigma_b}=(\psi_{\Sigma_b},\bar{\psi}^c_{\Sigma_b})^T$ is a Dirac spinor while ψ_{Σ_b} ($\bar{\psi}_{\Sigma_b}$) and $\psi^c_{\Sigma_b}$ ($\bar{\psi}^c_{\Sigma_b}$) are undotted (dotted) Weyl spinors. Concerning the $\mathbb{Z}_2$ symmetry, we assume the multiplets $(\Sigma_2,\psi_{\Sigma_2},F_{\Sigma_2})$ and $(\Sigma_1,\bar{\psi}^c_{\Sigma_1},F_{\Sigma_1})$ to be even and $(\Sigma_1^c,\psi_{\Sigma_1},F^c_{\Sigma_1})$ and $(\Sigma_2^c,\bar{\psi}^c_{\Sigma_2},F^c_2)$ to be odd, according to the orbifold action

$$\mathbb{Z}_2=\sigma_3|_{SU(2)_\Sigma}\otimes\gamma_5, \tag{4.1}$$

where σ_3 is acting over $SU(2)_\Sigma$ indices and γ_5 over Dirac indices. We denote their scalar KK modes as $\Sigma^{(n)}_{1,2}$ ($n\geq 0$) and $\Sigma^{c(n)}_{1,2}$ ($n\geq 1$).

This allows one to introduce the SS twists (q_R,q_Σ) that establish the transformation

$$\begin{bmatrix}\Sigma_1(x,y) & \Sigma_1^c(x,y)\\ \Sigma_2^c(x,y) & \Sigma_2(x,y)\end{bmatrix} = e^{iq_\Sigma\sigma_2 y}\sum_{n=0}^{\infty}\sqrt{\frac{2}{\pi}}\begin{bmatrix}\cos ny\Sigma_1^{(n)}(x) & \sin ny\Sigma_1^{c(n)}(x)\\ \sin ny\Sigma_2^{c(n)}(x) & \cos ny\Sigma_2^{(n)}(x)\end{bmatrix}e^{-iq_R\sigma_2 y}, \tag{4.2}$$

whose mode normalization is in analogy with Eq. (2.2). The pattern of the mass eigenvalues and the spectrum of the triplet is also similar to the ones in Eqs. (2.3) and (2.4). Indeed, applying the same normalization conventions, it turns out that the mass eigenstates $\sigma^{(n)}$ and $\Sigma^{(n)}$, with mass $q_R-q_\Sigma+n$ and $q_R+q_\Sigma+n$, respectively, are given by

$$\begin{aligned}\Sigma_1^{(n)}&=(\sigma^{(n)}+\sigma^{(-n)}+\Sigma^{(n)}+\Sigma^{(-n)})/2,\\ \Sigma_2^{(n)}&=(\sigma^{(n)}+\sigma^{(-n)}-\Sigma^{(n)}-\Sigma^{(-n)})/2,\\ \Sigma_1^{c(n)}&=(\sigma^{(-n)}-\sigma^{(n)}+\Sigma^{(-n)}-\Sigma^{(n)})/2,\\ \Sigma_2^{c(n)}&=(\sigma^{(n)}-\sigma^{(-n)}+\Sigma^{(-n)}-\Sigma^{(n)})/2,\end{aligned} \tag{4.3}$$

for $n\geq 1$, and by

$$\begin{aligned}\Sigma_1^{(0)}&=(\sigma^{(0)}+\Sigma^{(0)})/2,\\ \Sigma_2^{(0)}&=(\sigma^{(0)}-\Sigma^{(0)})/2,\end{aligned} \tag{4.4}$$

for $n=0$. The analogy also applies to the fermionic components of the triplet. Their tree-level mass spectrum is then similar to the one of the Higgsinos.

Only the even multiplets can have interactions on the $y=0$ brane, and the $N=1$ triplet supermultiplets that have such interactions are

$$\begin{aligned}\mathcal{T}_2&=(\Sigma_2,\psi_{\Sigma_2},F_{\Sigma_2}-\partial_5\Sigma_2^c),\\ \mathcal{T}_1&=(\Sigma_1^\dagger,\psi^c_{\Sigma_1},F^\dagger_{\Sigma_1}-\partial_5\Sigma_1^{c\dagger}).\end{aligned} \tag{4.5}$$

The generic brane superpotential involving these fields is

$$W=(\hat{\lambda}_1\mathcal{H}_1\cdot\mathcal{T}_1\mathcal{H}_2+\hat{\lambda}_2\mathcal{H}_1\cdot\mathcal{T}_2\mathcal{H}_2)\delta(y), \tag{4.6}$$

where $\hat{\lambda}_b$ are 5D Yukawa couplings with mass dimension equal to $-3/2$. In particular, in the superpotential no triplet tadpole or cubic terms are allowed by the gauge symmetry.

After integrating out the auxiliary fields we obtain the bosonic 4D Lagrangian

$$\begin{aligned}\mathcal{L}_4=&-\{H_1^\dagger(0)(\hat{\lambda}_1\partial_5\Sigma_1^{c\dagger}(0)+\hat{\lambda}_2\partial_5\Sigma_2^c(0))H_2(0)+\partial_5H_1^{c\dagger}(0)(\hat{\lambda}_1\Sigma_1^\dagger(0)+\hat{\lambda}_2\Sigma_2(0))H_2(0)\\ &+H_1^\dagger(0)(\hat{\lambda}_1\Sigma_1^\dagger(0)+\hat{\lambda}_2\Sigma_2(0))\partial_5H_2^c(0)+\text{H.c.}\}\\ &-\left\{\frac{1}{2}(\hat{\lambda}_1^2+\hat{\lambda}_2^2)\sum_A|H_1^\dagger(0)\tau_AH_2(0)|^2+|(\hat{\lambda}_1\Sigma_1^\dagger(0)+\hat{\lambda}_2\Sigma_2(0))H_2(0)|^2+|H_1^\dagger(0)(\hat{\lambda}_1\Sigma_1^\dagger(0)+\hat{\lambda}_2\Sigma_2(0))|^2\right\}\pi\delta(0),\end{aligned} \tag{4.7}$$

where τ_A are the Pauli matrices used in the definition $\Sigma_b\equiv\frac{1}{\sqrt{2}}T^b_A\tau_A$. By means of the notation

$$\sigma=\sum_{n=-\infty}^{\infty}\sigma^{(n)},\qquad \hat{\sigma}=\sum_{n=-\infty}^{\infty}(q_R-q_\Sigma+n)\sigma^{(n)}, \tag{4.8}$$

$$\Sigma=\sum_{n=-\infty}^{\infty}\Sigma^{(n)},\qquad \hat{\Sigma}=\sum_{n=-\infty}^{\infty}(q_R+q_\Sigma+n)\Sigma^{(n)}, \tag{4.9}$$

and the identities of Eq. (3.8) (with obvious replacements $h\to\sigma$ and $H\to\Sigma$), Eq. (4.7) reads

$$\mathcal{L}_4 = \Big\{\frac{1}{2\sqrt{2}}(\lambda_1-\lambda_2)[h^\dagger\hat{\sigma}h - H^\dagger\hat{\sigma}H + h^\dagger\hat{\Sigma}H - H^\dagger\hat{\Sigma}h - \hat{H}^\dagger(\sigma-\sigma^\dagger)h + \hat{h}^\dagger(\Sigma+\Sigma^\dagger)h + \hat{h}^\dagger(\sigma-\sigma^\dagger)H - \hat{H}^\dagger(\Sigma+\Sigma^\dagger)H]$$
$$+\frac{1}{2\sqrt{2}}(\lambda_1+\lambda_2)[h^\dagger\hat{\Sigma}h - H^\dagger\hat{\Sigma}H + h^\dagger\hat{\sigma}H - H^\dagger\hat{\sigma}h$$
$$+\hat{H}^\dagger(\sigma+\sigma^\dagger)H - \hat{h}^\dagger(\Sigma-\Sigma^\dagger)H + \hat{h}^\dagger(\sigma+\sigma^\dagger)h - \hat{H}^\dagger(\Sigma-\Sigma^\dagger)h] + \text{H.c.}\Big\}$$
$$-\frac{1}{4}[h^\dagger F_+ h + H^\dagger F_+ H + h^\dagger F_- H + H^\dagger F_- h]\pi\delta(0)$$
$$-\frac{\lambda_1^2+\lambda_2^2}{8}(|h|^4+|H|^4+6|h|^2|H|^2-6|h^\dagger H|^2-(h^\dagger H)^2-(H^\dagger h)^2)\pi\delta(0), \tag{4.10}$$

where $\lambda_b \equiv \hat{\lambda}_b/\sqrt{\pi^3}$ are the dimensionless 4D Yukawa coupling and $F_\pm$ is given by

$$F_\pm = \lambda_1^2[\sigma^\dagger+\Sigma^\dagger, \sigma+\Sigma]_\pm + \lambda_2^2[\sigma-\Sigma, \sigma^\dagger-\Sigma^\dagger]_\pm$$
$$+\lambda_1\lambda_2\{[\sigma-\Sigma, \sigma+\Sigma]_\pm + \text{H.c.}\}, \tag{4.11}$$

with $[x,y]_-$ and $[x,y]_+$ standing for the commutator and anticommutator operator, respectively. The decomposition

$$\sigma \equiv \sum_A t_A \tau_A/\sqrt{2} \tag{4.12}$$

and the identity $\tau^A_{ij}\tau^A_{k\ell} = 2\delta_{i\ell}\delta_{jk} - \delta_{ij}\delta_{k\ell}$ have also been used.

B. Quartic and quadratic terms of the lightest Higgs

From Eq. (4.10) we can determine the potential of $h^{(0)}$ at low energy. On top of the contribution $\pi\delta(0)(\lambda_1^2+\lambda_2^2)/8$, the low-energy quadratic coupling includes the threshold correction due to the heavy modes that are integrated out (for a didactic calculation of threshold effects see e.g. [39,40]). This relation is provided by the tree-level matching condition depicted in Fig. 6 where the identity (3.5) has been used pictorially. For $q_R = q_H$ the relation amounts to

$$\lim_{p\to 0}\sum_{n=-\infty}^{+\infty}\frac{(\lambda_1+\lambda_2)^2}{16}\left[1+\frac{(q_R+q_\Sigma+n)^2}{p^2-(q_R+q_\Sigma+n)^2}\right]|h^{(0)}|^4$$
$$+\lim_{p\to 0}\sum_{n=-\infty}^{+\infty}\frac{(\lambda_1-\lambda_2)^2}{16}\left[1+\frac{(q_R-q_\Sigma+n)^2}{p^2-(q_R-q_\Sigma+n)^2}\right]|h^{(0)}|^4$$
$$=\left[\frac{(\lambda_1+\lambda_2)^2}{16}\delta_{q_R+q_\Sigma,0}+\frac{(\lambda_1-\lambda_2)^2}{16}\delta_{q_R-q_\Sigma,0}\right]|h^{(0)}|^4. \tag{4.13}$$

For nonmaximal (and positive) twists the result is not vanishing only if $q_R = q_\Sigma$ and the whole contribution is due to the $n=0$ mode. Therefore, in order to achieve a sizable boost to the tree-level Higgs mass, we focus on the case $q_H = q_R = q_\Sigma \equiv \omega$ hereafter. The low-energy potential of $h^{(0)}$ is then given by

$$V_{\rm SM} = (m^2+\Delta_h m^2)|h^{(0)}|^2 + \left(\frac{(\lambda_1-\lambda_2)^2}{16}+\Delta\lambda\right)|h^{(0)}|^4+\cdots. \tag{4.14}$$

We then determine the $h^{(0)}$ quartic coupling at leading order in $\lambda_{1,2}$ and h_t, as in previous sections. The contribution depending on $\lambda_{1,2}$ appears at tree level while the latter appears at two loop and is given by Eq. (3.11) (see comments in Sec. III B). Once the observed EWSB is assumed, which in practice is equivalent to impose $m^2+\Delta_h m^2 \simeq -(88\ \text{GeV})^2$, the experimental measurement of the Higgs mass constrains $|\lambda_1-\lambda_2|$, R, and ω as shown in Fig. 7.[12]

The EWSB is actually achievable in the present scenario. For our choice of twists the tree-level squared mass m^2 is zero (see Sec. II). The radiative correction $\Delta_h m^2$ can be split as

$$\Delta_h m^2 = \Delta_g m^2 + \Delta_\lambda m^2, \tag{4.15}$$

with $\Delta_g m^2$ provided in Eq. (3.12). The contribution $\Delta_\lambda m^2$ comes from the interactions depending on the superpotential couplings $\lambda_{1,2}$. It is produced via the diagrams in Fig. 8 and results in

$$\Delta_\lambda m^2 = \frac{(\lambda_1-\lambda_2)^2+(\lambda_1+\lambda_2)^2}{2(4\pi)^4}\tilde{\Omega}(\omega), \tag{4.16}$$

with

[12]As we will discuss in Section IV D, $h^{(0)}$ mixes very mildly with the scalar triplet. The field $h^{(0)}$ is then the mass eigenstate that plays the role of the SM-like Higgs. In addition, because of the small mixing, only the squared-mass term of $h^{(0)}$ is relevant in the EWSB.

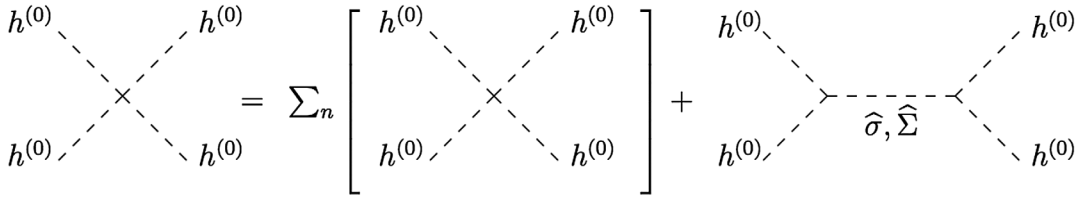

FIG. 6. Matching of the low-energy and high-energy $h^{(0)}$ four-point diagrams.

$$\tilde{\Omega}(\omega) = \Big\{ 2\zeta(3) - 4Li_3(e^{2i\pi\omega}) + 4i\cot(2\pi\omega)Li_4(e^{2i\pi\omega}) + Li_3(e^{4i\pi\omega}) - i\frac{2+3\cos(4\pi\omega)}{\sin(4\pi\omega)}Li_4(e^{4i\pi\omega}) + \text{H.c.}\Big\}(1/R)^2. \quad (4.17)$$

Figure 9 (left panel) displays the values of $\Delta_h m^2$ (solid line) and its contributions $\Delta_g m^2$ (dotted line) and $\Delta_\lambda m^2$ (dashed line) in units of $10^3 R^2$. The plot highlights the illustrative case $1/R = 2$ TeV. It assumes $|\lambda_1 - \lambda_2|$ fixed to reproduce the observed Higgs mass (cf. Fig. 7) and $\lambda_1 + \lambda_2$ set to zero to conservatively minimize the effect of $\Delta_\lambda m^2$ [see Eq. (4.16)]. We see that $\Delta_g m^2$ is positive for all values of ω, whereas $\Delta_\lambda m^2$ can be negative and sizable. In particular, at $\omega \lesssim 1/5$, $\Delta_h m^2$ is negative and the EWSB is achieved. Of course, the larger the value of $|\lambda_1 + \lambda_2|$ the more easily the EWSB is obtained. This is highlighted in the central panel of Fig. 9 presenting the contour lines of $R^2\Delta_h m^2$ in the $(\omega, |\lambda_1 + \lambda_2|)$ plane with still $1/R = 2$ TeV and $|\lambda_1 - \lambda_2|$ fulfilling the Higgs mass constraint. Along the (red) dotted line the condition $\Delta_h m^2 \approx -(88\ \text{GeV})^2$ for the observed EWSB is satisfied. The finding is generalized to any value of R in the right panel of Fig. 9 where the yellow area highlights the region of $(\omega, 1/R)$ providing $\Delta_h m^2 = -(88\ \text{GeV})^2$ with $|\lambda_1 + \lambda_2| \leq 2$ (the inner border corresponding to $\lambda_1 + \lambda_2 = 0$, the outer to $\lambda_1 + \lambda_2 = 2$). Also in this panel $|\lambda_1 - \lambda_2|$ is adjusted to reproduce the experimental Higgs mass.

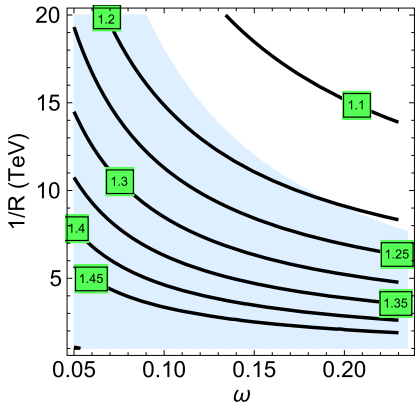

FIG. 7. Contour plot of values of $|\lambda_1 - \lambda_2|$ fixing the Higgs mass to its experimental value $m_h = 125$ GeV. Blue area is as in Fig. 1.

We conclude that in this 5D embedding the presence of triplets

(i) Enhances the tree-level Higgs quartic coupling in the effective theory and thus makes it easy to accommodate the 125 GeV Higgs mass constraint. This is essential for the naturalness of the model.

(ii) Triggers the EWSB by providing a sizable negative contribution to the squared-mass term of the SM-like

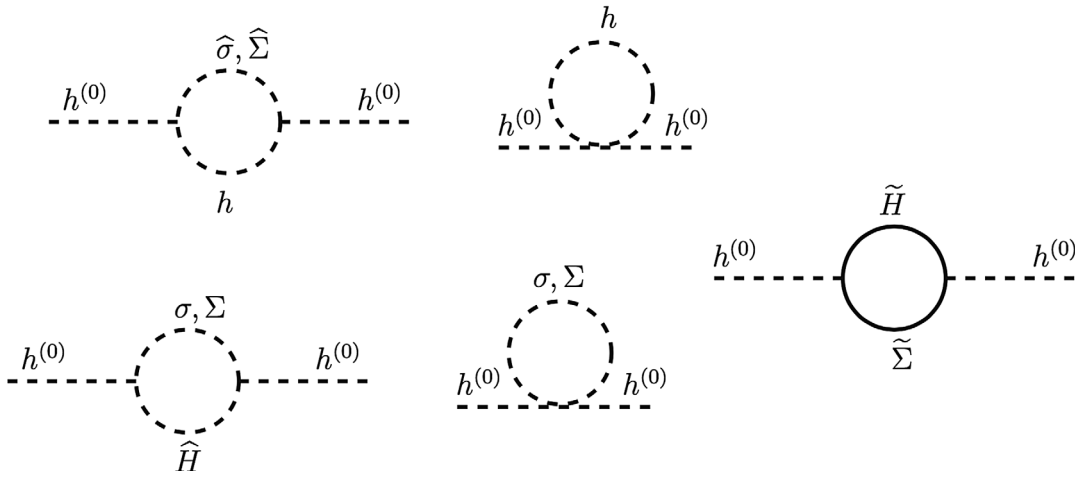

FIG. 8. Diagrams contributing to the mass term $\Delta_\lambda m^2$.

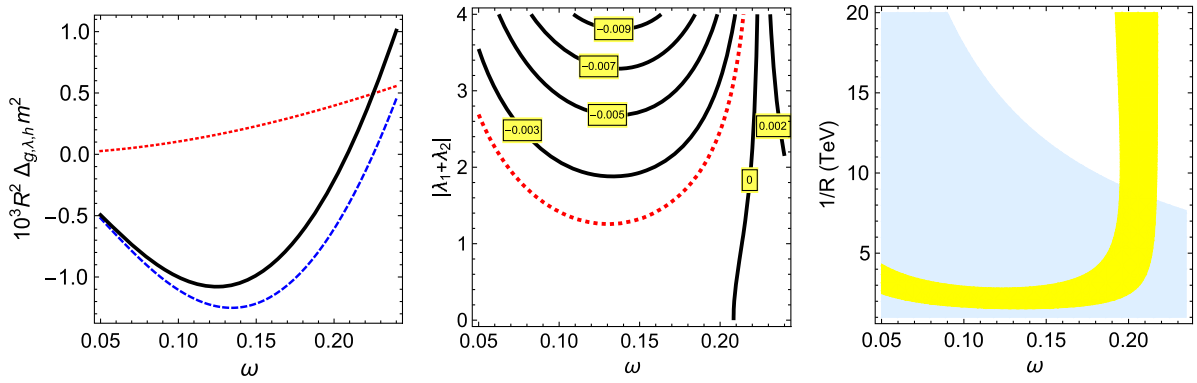

FIG. 9. Left panel: Plots of $\Delta_g m^2$ (red dotted line), $\Delta_\lambda m^2$ (blue dashed line), and their sum $\Delta_h m^2 = \Delta_g m^2 + \Delta_\lambda m^2$ (black solid line) as functions of ω in units of 10^3R^2 with $1/R = 2$ TeV and $\lambda_1 + \lambda_2 = 0$. Central panel: Contour plot of $R^2\Delta_h m^2$ in the $(\omega, |\lambda_1 + \lambda_2|)$ plane for $1/R = 2$ TeV. The correct EWSB with the experimentally observed 125 GeV Higgs mass happens along the dashed red line. Right panel: The parameter space of the $(\omega, 1/R)$ plane (yellow area) where the experimental EWSB with the correct Higgs mass is successfully achieved. Blue area is as in Fig. 1. In all panels $|\lambda_1 - \lambda_2|$ is fixed as in Fig. 7.

Higgs and, in a somewhat wide parameter region, generates the observed electroweak scale.

C. Triplet trilinear term and Higgs-triplet quartic coupling

Besides the squared mass of the triplet, there are other interactions that are important for the phenomenology of the model. In this section we focus on the triplet trilinear parameter and the Higgs-triplet quartic coupling by which we can determine the VEV and masses of the triplets (see Sec. IV D).

The trilinear A_λ term

$$\mathcal{L}_4 = \cdots - A_\lambda h^\dagger \sigma h + \text{H.c.} \tag{4.18}$$

is generated by a loop of Higgsinos and gauginos. It can be evaluated following the method employed for the stop mixing A_t in Ref. [21]. The result is given by

$$A_\lambda = \frac{3(\lambda_1+\lambda_2)\alpha_2}{16\sqrt{2}\pi^2} C_2^h [iLi_2(e^{-2i\pi\omega}) + \text{H.c.}]\frac{1}{R}, \tag{4.19}$$

where $C_2^h = 3/4$ is the quadratic Casimir of the Higgs doublet.

In order to calculate the quartic coupling between the light Higgs $h^{(0)}$ and the light triplet $\sigma^{(0)}$, we follow the procedure used in Sec. IV B. Specifically, we determine the tree-level matching of the Higgs-triplet interaction between the high-energy theory described in Eq. (4.10) and the low-energy one where only the (tree-level massless) zero modes exist. As previously stated, we focus on the case $\omega = q_R = q_H = q_\Sigma$. The nontrivial contributions are those corresponding to the vertices $|h^{(0)}|^2|(\sigma + \sigma^\dagger)^{(0)}|^2$, mediated by the propagation of $\hat{h}$, and $|h^{(0)}|^2|(\sigma - \sigma^\dagger)^{(0)}|^2$, mediated by the propagation of $\hat{H}$, depicted in Fig. 10. They can be evaluated by means of the identities

$$\lim_{p\to 0}\sum_n \frac{(\lambda_1 \pm \lambda_2)^2}{16}\left[1 + \frac{(q_R \mp q_H + n)^2}{p^2 - (q_R \mp q_H + n)^2}\right] = \frac{(\lambda_1 \pm \lambda_2)^2}{16}\delta_{q_R \mp q_H, 0}, \tag{4.20}$$

and they lead to the following quartic interaction term:

$$\mathcal{L}_{4D} = -\frac{(\lambda_1+\lambda_2)^2}{16} h^{(0)\dagger}[\sigma^{(0)} + \sigma^{(0)\dagger}, \sigma^{(0)} + \sigma^{(0)\dagger}]_+ h^{(0)} + \cdots = -\frac{(\lambda_1+\lambda_2)^2}{8} h^{(0)\dagger} h^{(0)} \sum_A [(t_R^A)^{(0)}]^2 + \cdots, \tag{4.21}$$

with $(t_R^A)^{(0)}$ defined as

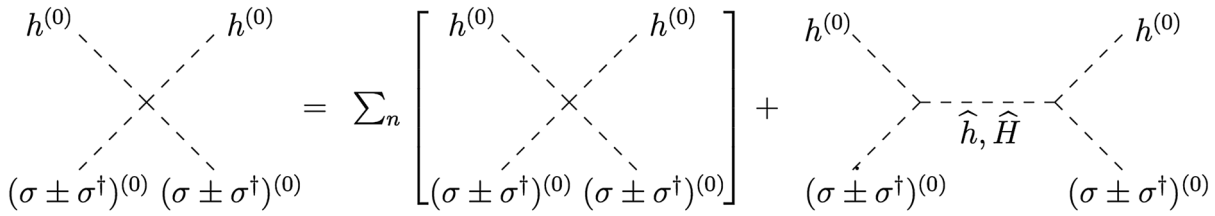

FIG. 10. High-energy diagrams leading to the low-energy quartic interactions between $h^{(0)}$ and $(\sigma \pm \sigma^\dagger)^{(0)}$, mediated by the propagation of $\hat{h}$ or $\hat{H}$, respectively.

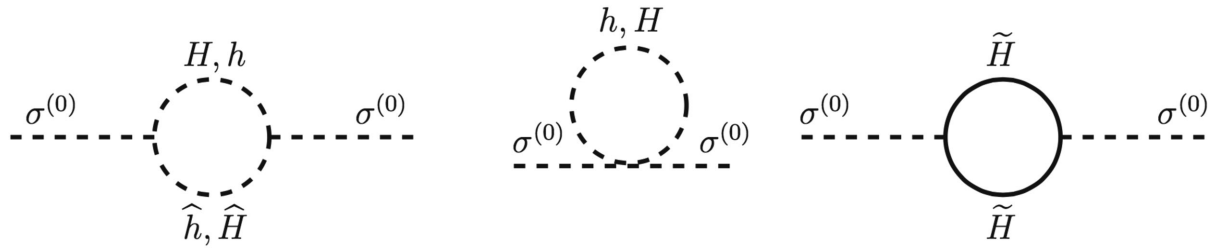

FIG. 11. Diagrams contributing to the mass term $\Delta m_\sigma^2|\sigma^{(0)}|^2$.

$$\sigma^{(0)} = \frac{(t_R^A)^{(0)} + i(t_I^A)^{(0)}}{2}\tau^A. \tag{4.22}$$

D. Triplet VEV and mass spectrum

The presence of the triplets has practically no effect on the mass spectrum of the 5D MSSM-like states but $h^{(0)}$. In fact, all modes of $\mathbb{H}_a$ except $h^{(0)}$ have large tree-level masses due to the SS mechanism, and the remaining MSSM-like fields do not have contact interaction with the triplets. The mass spectra shown in Figs. 1 and 2 then hold correct also in the present scenario [although only the (yellow) subregion highlighted in the right panel of Fig. 9 is consistent with the observed EWSB and 125 GeV $h^{(0)}$ mass for $|\lambda_1 + \lambda_2| \leq 2$]. The relevant difference between the spectra of the 5D MSSM and the triplet extension is then the masses of the additional fields.

With respect to the SS twists, the fermionic components of the triplets behave as the Higgsinos, and they are hence degenerate in mass with such fields. The scalar triplet $\sigma^{(0)}$ is instead insensitive to the SS mechanism at tree level (for $q_R = q_H = q_\Sigma$), and only its real part $\tau_A(t_R^A)^{(0)}/2$ receives a mass by means of the Higgs EWSB [cf. Eq. (4.21)]. However, this mass tends to be subdominant with respect to the one coming from the one-loop mass term $\Delta m_\sigma^2(\omega)|\sigma^{(0)}|^2$ that is produced by the diagrams in Fig. 11. This correction amounts to

$$\Delta m_\sigma^2 = \frac{3(\lambda_1+\lambda_2)^2}{(4\pi)^4}\Omega_\sigma^+(\omega) + \frac{6(\lambda_1-\lambda_2)^2}{(4\pi)^4}\Omega_\sigma^-(\omega), \tag{4.23}$$

with

$$\begin{aligned}\Omega_\sigma^-(\omega) &= \{-Li_3(e^{2i\pi\omega}) + i\cot(2\pi\omega)[-Li_4(e^{2i\pi\omega}) + Li_4(e^{4i\pi\omega})] + \text{H.c.}\}(1/R)^2,\\ \Omega_\sigma^+(\omega) &= \{2\zeta(3) - 2Li_3(e^{2i\pi\omega}) + Li_3(e^{4i\pi\omega}) + 2i\cot(2\pi\omega)Li_4(e^{2i\pi\omega})\\ &\quad - i\cot(4\pi\omega)Li_4(e^{4i\pi\omega}) + \text{H.c.}\}(1/R)^2.\end{aligned} \tag{4.24}$$

Therefore, after the EWSB, the squared masses of the zero modes of the real and imaginary parts of the complex triplets are, respectively, given by

$$(m_\sigma^R)^2 = \frac{(\lambda_1+\lambda_2)^2}{4}v^2 + \Delta m_\sigma^2, \tag{4.25}$$

$$(m_\sigma^I)^2 = \Delta m_\sigma^2. \tag{4.26}$$

The values of these masses as a function of ω and $1/R$ are displayed in the left panel of Fig. 12 where in the yellow area λ_1 and λ_2 are fixed as usual to satisfy the EWSB and Higgs mass constraints.

We now study the triplet VEV. When the Higgs breaks the electroweak symmetry, the trilinear interaction in Eq. (4.18) induces a tadpole term $\sim A_\lambda v^2(t_R^3)^{(0)}$. This in turn induces the VEV $\langle t_R^3\rangle \equiv \langle(t_R^3)^{(0)}\rangle$ which breaks custodial symmetry and affects the electroweak precision observable ρ as [41]

$$\Delta\rho = \frac{4\langle t_R^3\rangle^2}{v^2}, \tag{4.27}$$

which, using the (1σ) bound $\Delta\rho \lesssim 6\times 10^{-4}$, provides the corresponding bound $\langle t_R^3\rangle \lesssim 3$ GeV. Notice also the relation between the observables $\Delta\rho$ and T as given by $\Delta\rho = \alpha T$.[13]

The size of $\langle t_R^3\rangle$ is now obtained by considering the scalar potential involving the tadpole term and the squared mass in Eqs. (4.18) and (4.25). Its order of magnitude is $\mathcal{O}(A_\lambda v^2/(m_\sigma^R)^2)$ [34], and its precise value is shown in the right panel of Fig. 12 where we plot $\langle t_R^3\rangle$ as a function of ω and $1/R$ for $\lambda_1 - \lambda_2$ fixed by the experimental Higgs mass (cf. Fig. 7). The finding is displayed only in the (yellow)

[13]A more complete description will require other observables correlated with T, as S and U [42]. They will also be consistent with our model parameters as we will analyze at the end of Sec. IV E.

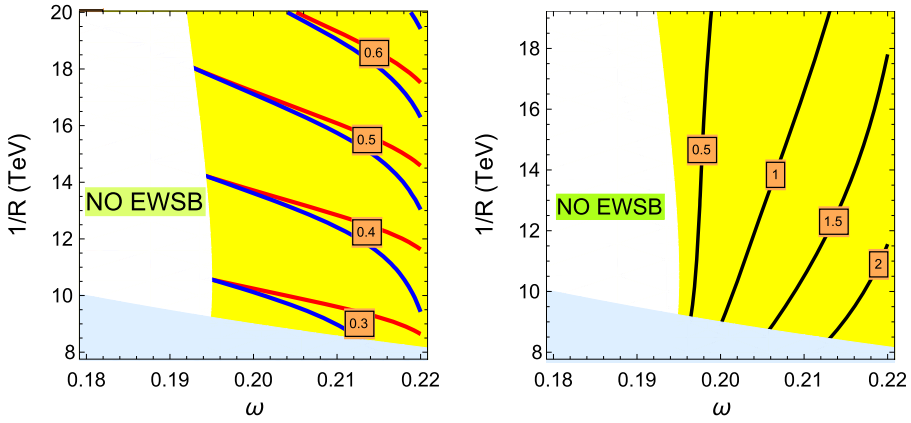

FIG. 12. Left panel: Contour plot of the real m_σ^R (blue curves) and imaginary m_σ^I (red curves) triplet masses. Right panel: Contour plot of the VEV (in GeV) that the triplet acquires due to the loop-induced trilinear term. In both panels it is assumed $|\lambda_1 + \lambda_2| < 2$ and the correct EWSB with a 125 GeV Higgs mass is achieved inside the yellow region. Blue areas are as in Fig. 1.

region where the observed EWSB can be achieved for $|\lambda_1 + \lambda_2| \leq 2$. The measurement of the ρ parameter, which imposes $\langle t_R^3 \rangle \lesssim 2$ GeV [34,41], provides no constraint on the model besides in the corner with $\omega \gtrsim 0.21$ and $1/R \lesssim 10$ TeV. In particular, along the left border of the yellow area, which corresponds to $(\lambda_1 + \lambda_2) = 0$, no trilinear term and thus no VEV of $(t_3^R)^{(0)}$ is generated. This border, although fine-tuned, is technically natural as λ_1 and λ_2 are supersymmetric parameters.

Finally, as a consistency check, we verify that the mixing between the $h^{(0)}$ and $(t_3^R)^{(0)}$ is tiny. Otherwise our criteria $\Delta_h m^2 \simeq -(88\ \text{GeV})^2$ and $m_h = 125$ GeV to accomplish the observed EWSB and Higgs mass constraints would be wrong. The mixing is sourced by the trilinear term in Eq. (4.18) after the EWSB. The mixing angle γ can be estimated as

$$\tan(2\gamma) \sim \frac{A_\lambda v}{(m_\sigma^R)^2 - m_h^2} \sim \frac{\langle t_3^R \rangle}{v}, \tag{4.28}$$

where in the last step the Higgs squared mass has been neglected in front of $(m_\sigma^R)^2$. The mixing is therefore fully negligible in the whole area compatible with the electroweak precision observables for which $\langle t_3^R \rangle \lesssim 3$ GeV.

To conclude, we provide some explicit values for an illustrative parameter scenario. We consider the benchmark point with $\omega = 3/14$ and $1/R = 14$ TeV. In this case the EWSB and Higgs mass constraints can be overcome with $\lambda_1 \simeq 1.1$ and $\lambda_2 \simeq 0.0$. The triplet VEV, which turns out to be $\langle t_3^R \rangle \simeq 1$ GeV, is compatible with the above ρ-parameter bound. The masses of the lightest modes corresponding to new physics are quoted in Table I. Some of them are within the reach of the LHC although they can be elusive to the standard searches as discussed in the next section.

E. The low-energy phenomenology

Below the energy scale of the bulk fields with masses $\mathcal{O}(\omega/R)$, the theory is described by the SM degrees of freedom plus the scalar triplet $\sigma^{(0)}$, and the third-generation squarks and slepton doublets.

In this setup the tau sneutrino ($\tilde{\nu}_\tau$) is the Light Supersymmetric Particle (LSP). The $\tilde{\nu}_\tau$ is not a good dark matter candidate as it would provide the observed relic abundance for a (small) mass range that is nevertheless ruled out by direct detection experiments [43]. In the remaining mass region, its relic density has to be somehow reduced. This is possible if the sneutrinos do not reach thermal equilibrium before their freeze-out, or an entropy injection occurs at late times (see e.g. [44,45]). Alternatively, decays such as $\tilde{\nu}_\tau \to \tau\bar{\tau}$ can provide the desired dilution. These could in principle be generated by operators like LLE that introduce a small R-parity violation.

The collider phenomenology of the left-handed stau ($\tilde{\tau}_L$) depends on its mass splitting with $\tilde{\nu}_\tau$. At tree level these fields are degenerate in mass, and only QED one-loop corrections break the degeneracy [46]. For the part of the parameter space that we are interested in, this splitting is at least $\mathcal{O}(100\ \text{MeV})$ and the lifetime of the stau is $\mathcal{O}(0.1\ \text{ns})$ or smaller, for which the ATLAS and CMS constraints on disappearing tracks can be interpreted as ruling out $m_{\tilde{\tau}} < 150$ GeV [47,48]. This low-mass range is also ruled out by other constraints, as we now see.

Even though the gluino is not part of the low-energy theory, the most robust constraint to the parameter space of

TABLE I. A sample of new-physics masses (in GeV) for $1/R = 14$ TeV and $\omega/R = 3$ corresponding to $\omega \simeq 0.21$. The symbol $m_{\tilde{f}_{1,2}}$ represents the mass of all sfermions of the first and second generations. The radiative corrections are included only for the masses of the last five columns.

$m_{\tilde{f}_{1,2}} = m_{\tilde{\tau}_R} = M_a$ $= m_{\tilde{H}} = m_{\tilde{\Sigma}}$	$m_H = m_\Sigma$	$m_{\tilde{t}_L}$	$m_{\tilde{t}_R}$	$m_{\tilde{\tau}_L} = m_{\tilde{\nu}_\tau}$	m_σ^R	m_σ^I
3000	6000	970	900	420	450	440

the model is provided by the gluino direct searches. From early 13 TeV data, ATLAS and CMS set the bound $m_{\tilde{g}} \gtrsim 1.8$ TeV [14,15]. Since the whole spectrum mostly depends on just two parameters, ω and $1/R$, and in particular $m_{\tilde{g}} = \omega/R$, the gluino mass bound constrains the low energy theory. The excluded region corresponds to the blue areas in Figs. 1, 2, 3, 7, 9, and 12. In particular, as highlighted in Figs. 1 and 12, the gluino bound forces the mass of the stops and sbottoms to be roughly above 550 GeV and the scalar triplet, stau, and tau sneutrino to be heavier than around 250 GeV. Of course, by excluding heavier gluino masses we will also be able to set stronger bounds on third-generation squarks, the triplet, and the stau doublet. However, the way in which the tree-level generated gaugino masses scale with $1/R$ is different from how the radiatively generated light states do. Even a 3 TeV bound on gluino masses will not be able to exclude stops at around 1 TeV nor stau and triplet masses around 500 GeV (see Table I). Hence it is worth studying also the phenomenology of these particles.

As we are dealing with a heavy LSP with a mass typically above 300 GeV, the LHC bounds from stop searches are very mild or even absent [49]. In addition, considering usual bounds is a conservative assumption; in this model the topology of the stop decays is different from what is expected in MSSM-like scenarios. Because the stop is lighter than all neutralinos and charginos, it decays to off-shell states such that the final signature is a multibody decay for which the current stop bounds can be very much softened [50]. Bounds on sbottoms are more severe than those on stops (for LSP masses below 400 GeV, ATLAS and CMS exclude sbottom masses up to 900 GeV [51,52]) but they suffer from the same softening mentioned above for stops. In this sense, in the present model the phenomenology of the third-generation squark is similar to the one analyzed in Ref. [25].

Direct detection of the scalar triplet is challenging. The triplet does not mix with the Higgs, is fermiophobic, and gets a very small VEV; thus, production mechanisms such as gluon fusion or vector boson fusion are of no use. Multilepton searches can be employed, but these are able to constrain only the parameter space where the triplet is very light ($\lesssim$200 GeV) and acquires a VEV close to the ρ-parameter bound [38]. Alternatively, by using Drell-Yan double production one can constrain fermiophobic scalars that do not acquire a sizable VEV and have no other way to be produced [53]. Because of kinematics, the Drell-Yan process gets weaker for larger triplet masses, and to rule out masses above 250 GeV one would need a 100 TeV collider in which the Drell-Yan production cross section is enhanced.

Finally, modifications to the loop-induced decay rates $\Gamma(g \to \gamma\gamma)$ and $\Gamma(h \to Z\gamma)$ could be generated by the new charged scalars of the triplet or the stau. These can result in deviations of the Higgs signal strengths; however, they will be very suppressed as very light masses ($\lesssim$200 GeV) or large couplings, $\mathcal{O}(1)$, are needed to produce a significant enhancement in the Higgs decay rates. Similarly, the loop level contributions to the S and T parameters are very small as the gluino bound already forbids the new low-energy states to be below 300 GeV, where significant modifications could be generated. We have explicitly calculated these using the results from Ref. [54] and found no significant contributions in the parts of the $(\omega, 1/R)$ plane which are not already excluded by other measurements. In particular, we find that $T^{1-\text{loop}} < 0.02$ and $S^{1-\text{loop}} < 0.002$, well inside their experimental bounds [41].

V. CONCLUSIONS

In the present paper we have explored extra dimensions as a way to minimize the fine-tuning triggered by the LHC constraints on minimal supersymmetric extensions of the Standard Model. We have performed our study focusing on five-dimensional supersymmetric embeddings, with the fifth dimension compactified on an orbifold and $N = 1$ supersymmetry breaking of the Scherk-Schwarz type.

The Scherk-Schwarz paradigm for SUSY breaking has been extensively explored in the literature and is able to provide interesting ways out for some of the shortcomings of conventional scenarios of softly broken supersymmetry. For instance, the μ/B_μ problem is avoided as a large Higgsino mass arises without any dimensional parameter in the superpotential. The spectrum exhibits a pattern made of compressed sectors, each one hierarchically separated in mass from the others by multiples of ω/R or $1/R$ (with ω and R being, respectively, the Scherk-Schwarz twist and the size of the extra dimension). In this way the first- and second-generation sfermions are naturally much heavier than the third-generation ones, in agreement with flavor constraints. Moreover, due to the absence of large effects in the renormalization-group evolution of the parameters, the framework is also free of the gluino-sucks problem and sub-TeV third-generation squarks are easily accommodated. The two main drawbacks of the paradigm come when considering the electroweak symmetry breaking and the experimentally measured Higgs mass, both not achievable in minimal realizations of Scherk-Schwarz supersymmetry breaking.

The present paper proves that these two problems are not generic obstacles in Scherk-Schwarz scenarios. It shows that, for instance, both issues can be solved in an extension with $Y = 0$ $SU(2)_L$ triplets propagating in the bulk. It turns out that such triplets both provide radiative corrections triggering the electroweak symmetry breaking and enhance the tree-level Higgs mass, so that the 125 GeV mass is adjusted more naturally.

Because of the mass hierarchy between fields that propagate in the bulk and fields localized in the brane, most of the new-physics sector is decoupled from electroweak-scale processes, in agreement with experiments. However, some superpartners, tightly linked to naturalness

and/or properties of the Scherk-Schwarz twists, have to be light and populate the low-energy particle content of the theory, which eventually consists of the Standard Model degrees of freedom plus a scalar triplet, the third-generation of squarks, and the doublet of sleptons. The presence of the right-handed staus in the light spectrum that we have avoided in the paper is really optional. Depending on the choice, the LSP can be the right-handed stau or the tau sneutrino. The latter is preferable to avoid the strong constraints on charged LSPs.

Since gluino bounds are robust and quite generic, the most stringent constraint to the model comes from gluino searches. Nevertheless, other experimental signals could be used to test it. In the short term, searches for disappearing tracks or fermiophobic scalars are the most promising for probing part of the parameter space. Searches for the third generation of squarks are also important, but it is challenging to apply their bounds to the present scenario where squarks have multibody decays [50]. We leave for the future the reinterpretation of these bounds in terms of the parameter space of the model.

ACKNOWLEDGMENTS

We thank ICTP-SAIFR for the kind hospitality during the first stages of this article. The work of A. D. is partly supported by the National Science Foundation under Grant No. PHY-1520966. The work of G. N. is supported by the Swiss National Science Foundation (SNF) under Grant No. 200020-155935. The work of M. G.-P. and M. Q. is partly supported by MINECO under Grant No. CICYT-FEDER-FPA2014-55613-P, by the Severo Ochoa Excellence Program of MINECO under Grant No. SO-2012-0234, and by Secretaria d'Universitats i Recerca del Departament d'Economia i Coneixement de la Generalitat de Catalunya under Grant No. 2014 SGR 1450. The work of M. Q. was also partly supported by CNPq PVE fellowship Project No. 405559/2013-5.

[1] G. Aad (ATLAS Collaboration), Search for supersymmetry at $\sqrt{s} = 13$ TeV in final states with jets and two same-sign leptons or three leptons with the ATLAS detector, Eur. Phys. J. C **76**, 259 (2016).

[2] V. Khachatryan (CMS Collaboration), Search for supersymmetry in pp collisions at $\sqrt{(s)} = 13$ TeV in the single-lepton final state using the sum of masses of large-radius jets, J. High Energy Phys. 08 (2016) 122.

[3] G. Aad (ATLAS Collaboration), Search for an additional, heavy Higgs boson in the $H \to ZZ$ decay channel at $\sqrt{s} =$ 8 TeV in pp collision data with the ATLAS detector, Eur. Phys. J. C **76**, 45 (2016).

[4] V. Khachatryan (CMS Collaboration), Searches for a heavy scalar boson H decaying to a pair of 125 GeV Higgs bosons hh or for a heavy pseudoscalar boson A decaying to Zh, in the final states with $h \to \tau\tau$, Phys. Lett. B **755**, 217 (2016).

[5] J. L. Feng, K. T. Matchev, and T. Moroi, Focus points and naturalness in supersymmetry, Phys. Rev. D **61**, 075005 (2000).

[6] J. L. Feng, K. T. Matchev, and D. Sanford, Focus point supersymmetry redux, Phys. Rev. D **85**, 075007 (2012).

[7] A. Delgado, M. Quiros, and C. Wagner, General focus point in the MSSM, J. High Energy Phys. 04 (2014) 093.

[8] A. Delgado, M. Quiros, and C. Wagner, Focus point in the light stop scenario, Phys. Rev. D **90**, 035011 (2014).

[9] I. Masina, G. Nardini, and M. Quiros, Electroweak vacuum stability and finite quadratic radiative corrections, Phys. Rev. D **92**, 035003 (2015).

[10] A. Heister (ALEPH Collaboration), Search for charginos nearly mass degenerate with the lightest neutralino in $e+$ $e-$ collisions at center-of-mass energies up to 209-GeV, Phys. Lett. B **533**, 223 (2002).

[11] G. Aad (ATLAS Collaboration), Search for the direct production of charginos, neutralinos and staus in final states with at least two hadronically decaying taus and missing transverse momentum in pp collisions at $\sqrt{s} = 8$ TeV with the ATLAS detector, J. High Energy Phys. 10 (2014) 096.

[12] V. Khachatryan (CMS Collaboration), Searches for electroweak production of charginos, neutralinos, and sleptons decaying to leptons and W, Z, and Higgs bosons in pp collisions at 8 TeV, Eur. Phys. J. C **74**, 3036 (2014).

[13] G. Isidori, Y. Nir, and G. Perez, Flavor physics constraints for physics beyond the standard model, Annu. Rev. Nucl. Part. Sci. **60**, 355 (2010).

[14] ATLAS Collaboration, Search for pair-production of gluinos decaying via stop and sbottom in events with b-jets and large missing transverse momentum in $\sqrt{s} = 13$ TeV pp collisions with the ATLAS detector, CERN Technical Report No. ATLAS-CONF-2015-067, 2015.

[15] CMS Collaboration, Search for new physics in the all-hadronic final state with the MT2 variable, CERN Technical Report No. CMS-PAS-SUS-15-003, 2015.

[16] M. Aaboud (ATLAS Collaboration), Search for top squarks in final states with one isolated lepton, jets, and missing transverse momentum in $\sqrt{s} = 13$ TeV pp collisions with the ATLAS detector, Phys. Rev. D **94**, 052009 (2016).

[17] S. P. Martin and M. T. Vaughn, Two loop renormalization group equations for soft supersymmetry breaking couplings, Phys. Rev. D **50**, 2282 (1994); **78**, 039903(E) (2008).

[18] I. Antoniadis, A possible new dimension at a few TeV, Phys. Lett. B **246**, 377 (1990).

[19] A. Pomarol and M. Quiros, The standard model from extra dimensions, Phys. Lett. B **438**, 255 (1998).

[20] I. Antoniadis, S. Dimopoulos, A. Pomarol, and M. Quiros, Soft masses in theories with supersymmetry breaking by TeV compactification, Nucl. Phys. **B544**, 503 (1999).
[21] A. Delgado, A. Pomarol, and M. Quiros, Supersymmetry and electroweak breaking from extra dimensions at the TeV scale, Phys. Rev. D **60**, 095008 (1999).
[22] J. Scherk and J. H. Schwarz, How to get masses from extra dimensions, Nucl. Phys. **B153**, 61 (1979).
[23] M. Quiros, New ideas in symmetry breaking, in *Summer Institute 2002 (SI 2002), Fuji-Yoshida, Japan, 2002*, pp. 549–601, 2003.
[24] S. Dimopoulos, K. Howe, and J. March-Russell, Maximally Natural Supersymmetry, Phys. Rev. Lett. **113**, 111802 (2014).
[25] I. G. Garcia, K. Howe, and J. March-Russell, Natural Scherk-Schwarz theories of the weak scale, J. High Energy Phys. 12 (2015) 005.
[26] T. Cohen, N. Craig, H. K. Lou, and D. Pinner, Folded supersymmetry with a twist, J. High Energy Phys. 03 (2016) 196.
[27] G. Aad (ATLAS, CMS Collaborations), Measurements of the Higgs boson production and decay rates and constraints on its couplings from a combined ATLAS and CMS analysis of the LHC pp collision data at $\sqrt{s} = 7$ and 8 TeV, J. High Energy Phys. 08 (2016) 045.
[28] CMS Collaboration, Search for heavy stable charged particles with 12.9 fb^{-1} of 2016 data, CERN Technical Report No. CMS-PAS-EXO-16-036, 2016.
[29] E. A. Mirabelli and M. E. Peskin, Transmission of supersymmetry breaking from a four-dimensional boundary, Phys. Rev. D **58**, 065002 (1998).
[30] M. Carena, J. R. Espinosa, M. Quiros, and C. E. M. Wagner, Analytical expressions for radiatively corrected Higgs masses and couplings in the MSSM, Phys. Lett. B **355**, 209 (1995).
[31] J. R. Espinosa and M. Quiros, Upper bounds on the lightest Higgs boson mass in general supersymmetric Standard Models, Phys. Lett. B **302**, 51 (1993).
[32] J. R. Espinosa and M. Quiros, Higgs triplets in the supersymmetric standard model, Nucl. Phys. **B384**, 113 (1992).
[33] S. Di Chiara and K. Hsieh, Triplet extended supersymmetric Standard Model, Phys. Rev. D **78**, 055016 (2008).
[34] A. Delgado, G. Nardini, and M. Quiros, Large diphoton Higgs rates from supersymmetric triplets, Phys. Rev. D **86**, 115010 (2012).
[35] A. Delgado, G. Nardini, and M. Quiros, A light Supersymmetric Higgs sector hidden by a standard model-like Higgs, J. High Energy Phys. 07 (2013) 054.
[36] P. Bandyopadhyay, K. Huitu, and A. Sabanci, Status of $Y = 0$ triplet Higgs with supersymmetry in the light of $\sim$125 GeV Higgs discovery, J. High Energy Phys. 10 (2013) 091.
[37] C. Arina, V. Martin-Lozano, and G. Nardini, Dark matter versus $h \to \gamma\gamma$ and $h \to \gamma Z$ with supersymmetric triplets, J. High Energy Phys. 08 (2014) 015.
[38] P. Bandyopadhyay, K. Huitu, and A. Sabanci Keceli, Multilepton signatures of the triplet like charged Higgs at the LHC, J. High Energy Phys. 05 (2015) 026.
[39] M. Carena, G. Nardini, M. Quiros, and C. E. M. Wagner, The effective theory of the light stop scenario, J. High Energy Phys. 10 (2008) 062.
[40] P. Draper and H. Rzehak, A review of Higgs mass calculations in supersymmetric models, Phys. Rep. **619**, 1 (2016).
[41] K. A. Olive (Particle Data Group Collaboration), Review of particle physics, Chin. Phys. C **38**, 090001 (2014).
[42] M. E. Peskin and T. Takeuchi, Estimation of oblique electroweak corrections, Phys. Rev. D **46**, 381 (1992).
[43] T. Falk, K. A. Olive, and M. Srednicki, Heavy sneutrinos as dark matter, Phys. Lett. B **339**, 248 (1994).
[44] G. Gelmini and P. Gondolo, DM production mechanisms, *Particle Dark Matter*, edited by G. Bertone (Cambridge University Press, Cambridge, UK, 2010), pp. 121–141.
[45] G. Nardini and N. Sahu, Re-reheating, late entropy injection and constraints from baryogenesis scenarios, arXiv:1109.2829.
[46] M. Cirelli, N. Fornengo, and A. Strumia, Minimal dark matter, Nucl. Phys. **B753**, 178 (2006).
[47] G. Aad (ATLAS Collaboration), Search for charginos nearly mass degenerate with the lightest neutralino based on a disappearing-track signature in pp collisions at $\sqrt{s} = 8$ TeV with the ATLAS detector, Phys. Rev. D **88**, 112006 (2013).
[48] V. Khachatryan (CMS Collaboration), Search for disappearing tracks in proton-proton collisions at $\sqrt{s} = 8$ TeV, J. High Energy Phys. 01 (2015) 096.
[49] G. Aad (ATLAS Collaboration), ATLAS Run 1 searches for direct pair production of third-generation squarks at the Large Hadron Collider, Eur. Phys. J. C **75**, 510 (2015); Eur. Phys. J. C **76**, 153(E) (2016).
[50] D. S. M. Alves, J. Liu, and N. Weiner, Hiding missing energy in missing energy, J. High Energy Phys. 04 (2015) 088.
[51] ATLAS Collaboration, Search for Bottom Squark Pair Production with the ATLAS Detector in proton-proton Collisions at $\sqrt{s} = 13$ TeV, CERN Technical Report No. ATLAS-CONF-2015-066, 2015.
[52] CMS Collaboration, Search for direct production of bottom and light top squark pairs in proton-proton collisions at $\sqrt{s} = 13$ TeV, CERN Technical Report No. CMS-PAS-SUS-16-001, 2016.
[53] A. Delgado, M. Garcia-Pepin, M. Quiros, J. Santiago, and R. Vega-Morales, Diphoton and diboson probes of fermiophobic Higgs bosons at the LHC, J. High Energy Phys. 06 (2016) 042.
[54] Z. U. Khandker, D. Li, and W. Skiba, Electroweak Corrections from Triplet Scalars, Phys. Rev. D **86**, 015006 (2012).